Supplemental Information

Sec71 functions as a GEF for the small GTPase Arf1 to govern dendrite pruning of *Drosophila* sensory neurons

Yan Wang[1,2], Heng Zhang[1], Meng Shi[3], Yih-Cherng Liou[1,2], Lei Lu[3], Fengwei Yu[1,2,4,*]

Figure S1

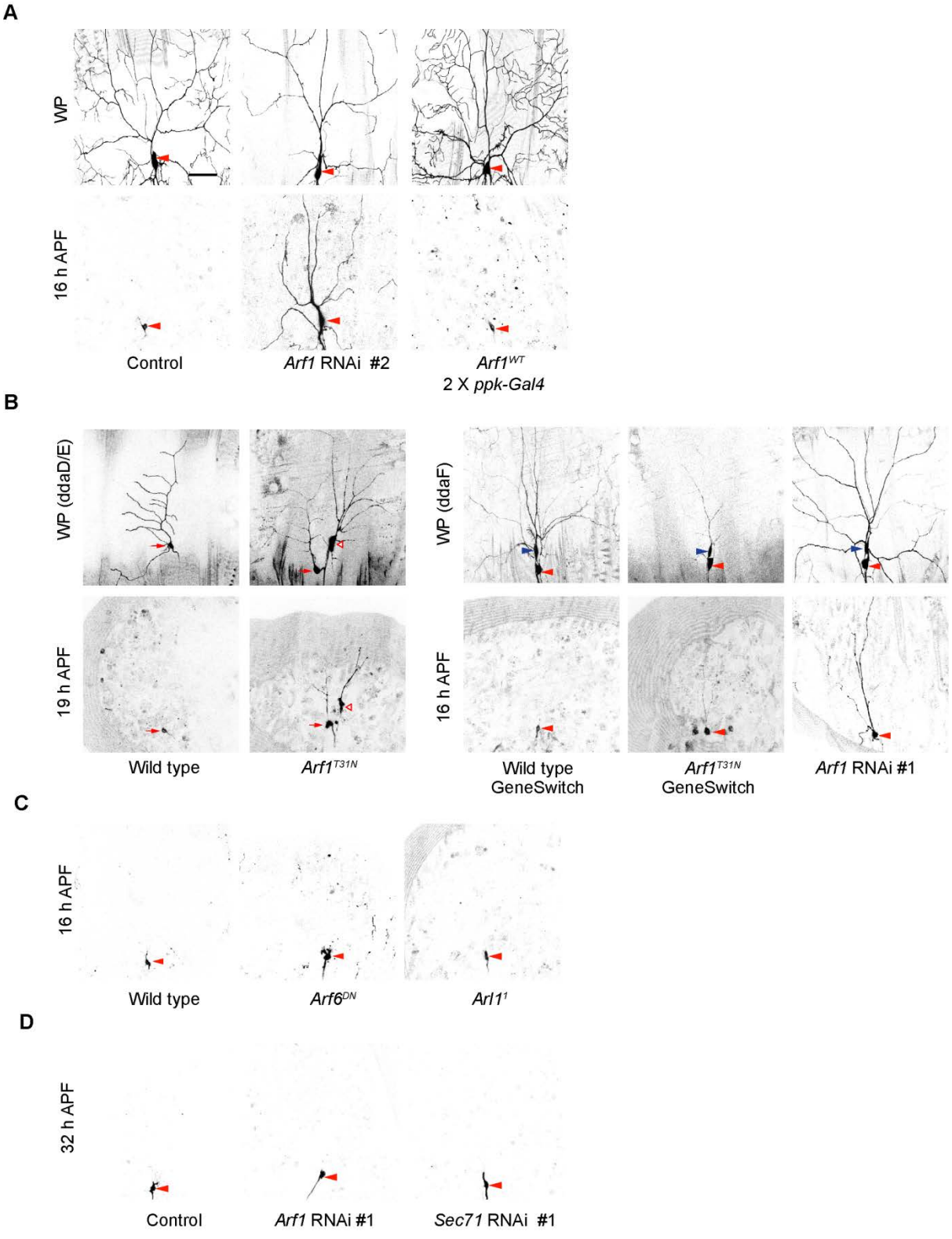

Figure S1. Arf1 is required for dendrite pruning in da sensory neurons.

(A-D) Live confocal images of ddaC or ddaD/E neurons expressing mCD8-GFP at WP stage, 16 h or 19 h APF. (A) While the control neurons that expressed an irrelevant RNAi line pruned all the dendrites, ddaC neurons overexpressing *Arf1* RNAi #2 by *ppk-Gal4* exhibited simple dendrite arbors at WP stage and dendrite pruning defects at 16 h APF. $Arf1^{WT}$-expressing ddaC neurons by two copies of *ppk-Gal4* driver at WP stage exhibited normal dendrite morphology and pruned their larval dendrites at 16 h APF. Red arrowheads point to the ddaC somas. (B) While wild-type class I ddaD/ddaE neurons pruned their larval dendrites at 19 h APF, $Arf1^{T31N}$ mutant ddaD and ddaE clones retained some of their larval dendrites at the same time point. Red arrows point to the ddaD somas and open arrowheads to the ddaE somas. Wild-type ddaF underwent apoptosis and disappeared at 16 h APF. Similarly, $Arf1^{T31N}$ ddaF labelled by GSG2295-driven mCD8-GFP and *Arf1* RNAi #1 mutant ddaF neurons were also removed at 16 h APF. Red arrowheads point to the ddaC somas, and blue arrowheads point to the ddaF somas. (C) Dendrites of $Arf6^{DN}$-expressing ddaC neurons and $Arl1^{1}$ MARCM ddaC clones (n=5) were pruned at 16 h APF, similar to the wild-type controls. (D) Similar to the control RNAi-expressing ddaC neurons, ddaC neurons overexpressing *Arf1* RNAi #1 (n=14) and *Sec71* RNAi #1 (n=12) by *ppk-Gal4* pruned all the dendrites at 32 h APF. Red arrowheads point to the ddaC somas. Scale bar in (A) represents 50 μm. See genotypes in Supplemental list of fly strains.

Figure S2

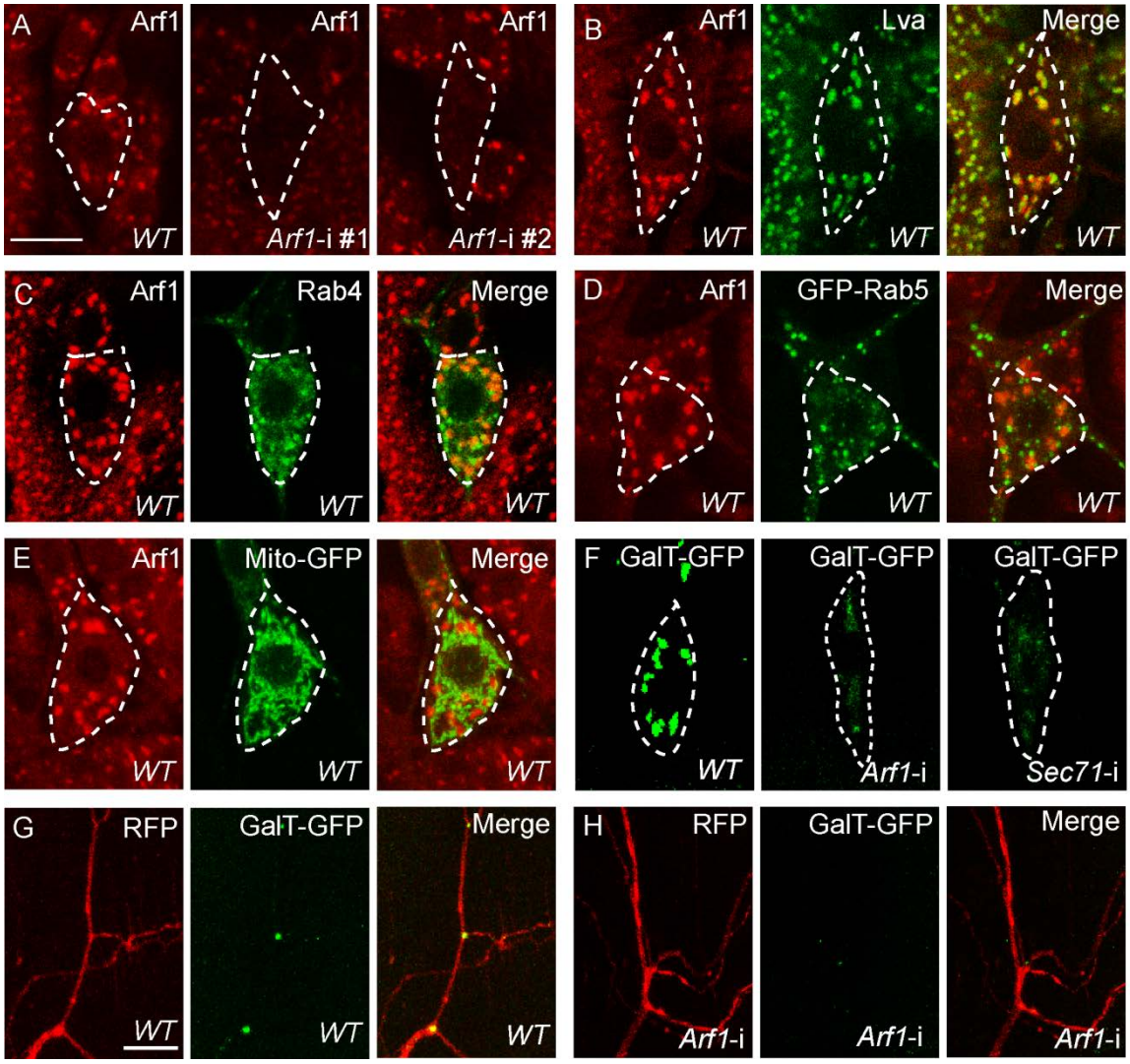

Figure S2. Arf1 does not localize on endosomes and mitochondria in ddaC sensory neurons.

(A-E) Confocal images of wild-type and mutant ddaC neurons at the late wL3 stage immunostained with anti-Arf1 or anti-Lva. ddaC somas are marked by dashed lines. (A) While Arf1 exhibited punctate structures in wild-type ddaCs, Arf1 staining in *Arf1* #1 RNAi or *Arf1* #2 RNAi ddaC neurons was abolished, verifying the specificity of the anti-Arf1 antibody. (B) Arf1-positive puncta (in red) largely co-localized with the Golgi marker Lva (in green) in wild-type ddaC somas. (C) Arf1-positive puncta (in red) did not overlap with the recycling endosomal marker Rab4-mRFP (in green) in wild-type ddaC neurons. (D) Arf1-positive puncta (in red) did not overlap with the early endosomal marker GFP-Rab5 (in green) in wild-type ddaC neurons. (E) Arf1-positive puncta (in red) did not overlap with the mitochondrial marker Mito-GFP (in green) in wild-type ddaC neurons. (F-H) Live confocal images of ddaC neurons expressing GalT-GFP and mCD8-RFP at WP stage. (F) GalT-GFP signals in soma were largely disrupted in *Arf1* RNAi and *Sec71* RNAi-expressing ddaC neurons. (G-H) GalT-GFP-positive dendritic Golgi outposts were disrupted in *Arf1* RNAi ddaC neurons (H), compared to those in wild-type ddaC neurons (G). Scale bars in (A) and (G) represent 10 μm. See genotypes in Supplemental list of fly strains.

Figure S3

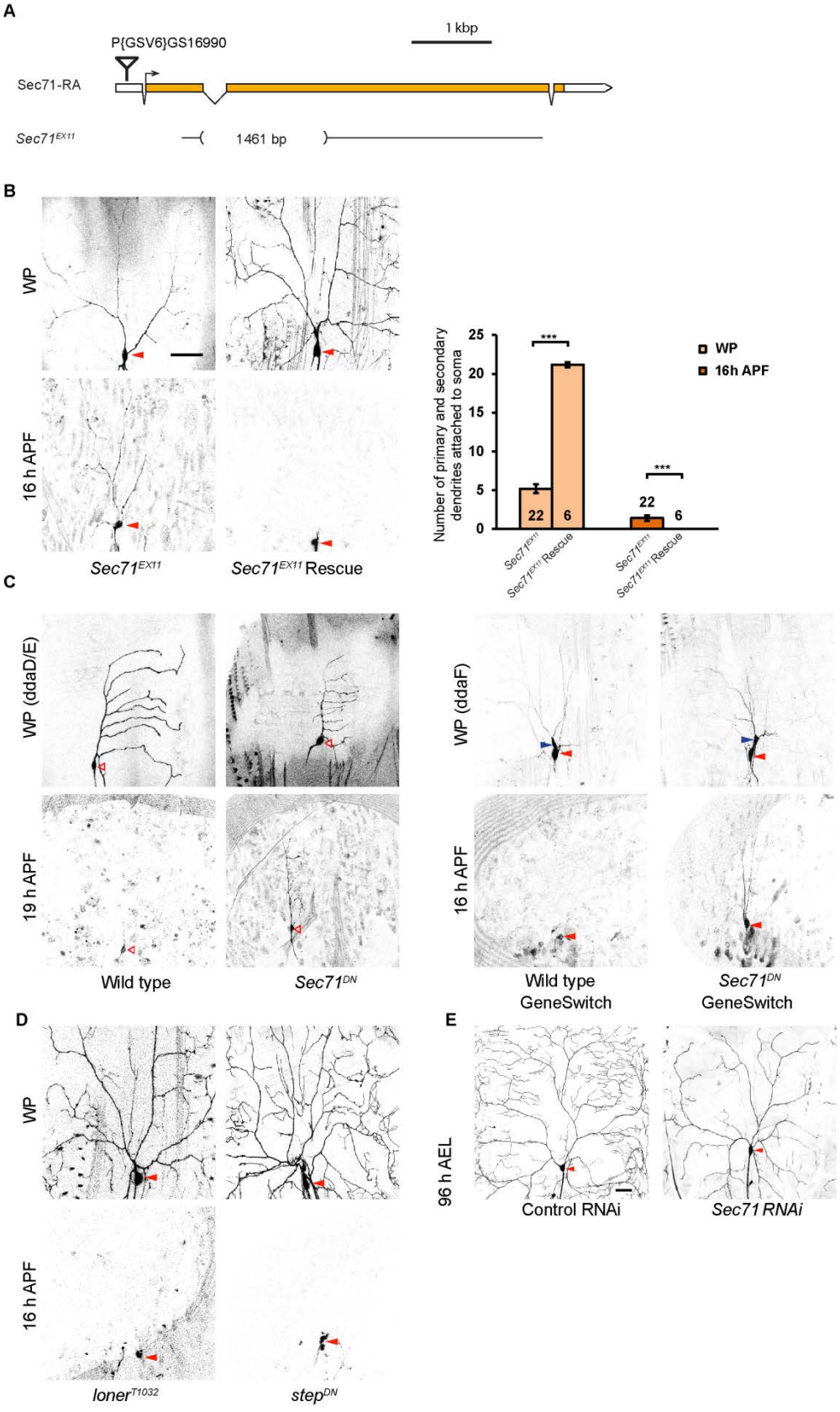

Figure S3. Sec71 is crucial for the regulation of dendrite pruning in sensory neurons.

(A) A schematic diagram of the *Sec71* gene and the deleted region of the $Sec71^{Ex11}$ mutant. The P-element insertion P{GSV6}GS16990, which is inserted in the first exon of the gene, was used to generate imprecise excision mutants. The start site of the *Sec71* open reading frame is shown in an arrow. (B-E) Live confocal images of ddaC or ddaD/E neurons expressing mCD8-GFP at wL3, WP, 16 h or 19 h APF stages. (B) $Sec71^{Ex11}$ MARCM ddaC clones exhibited simple arbors at WP stage and pruning defects at 16 h APF. Both dendrite morphological defects and pruning defects could be rescued by expressing full-length Sec71 protein in $Sec71^{Ex11}$ MARCM ddaC neurons. Red arrowheads point to the ddaC somas. Quantification of the average number of primary and secondary ddaC dendrites. Error bars represent S.E.M.. ***$p < 0.001$ as assessed by two-tailed Student's T test. (C) While wild-type class I ddaD/ddaE neurons pruned their larval dendrites at 19 h APF, $Sec71^{DN}$ ddaD or ddaE MARCM mutant clones failed to prune their larval dendrites at 19 h APF. Open arrowheads point to the ddaE somas. Wild-type ddaFs underwent apoptosis and were gone by 16 h APF. Similarly, $Sec71^{DN}$ ddaFs labelled by GSG2295-driven mCD8-GFP also underwent apoptosis by 16 h APF. Red arrowheads point to the ddaC somas, and blue arrowheads point to the ddaF somas. (D) Dendrites of $loner^{T1032}$ MARCM and $Step^{DN}$-expressing ddaC neurons were removed by 16 h APF. (E) While control RNAi-expressing ddaC neurons exhibited complex arbors at 96 h AEL, *Sec71* RNAi-expressing ddaC neurons exhibited simplified arbors. Red arrowheads point to the ddaC somas. Scale bar in (B) and (E) represents 50 μm. See genotypes in Supplemental list of fly strains.

Figure S4

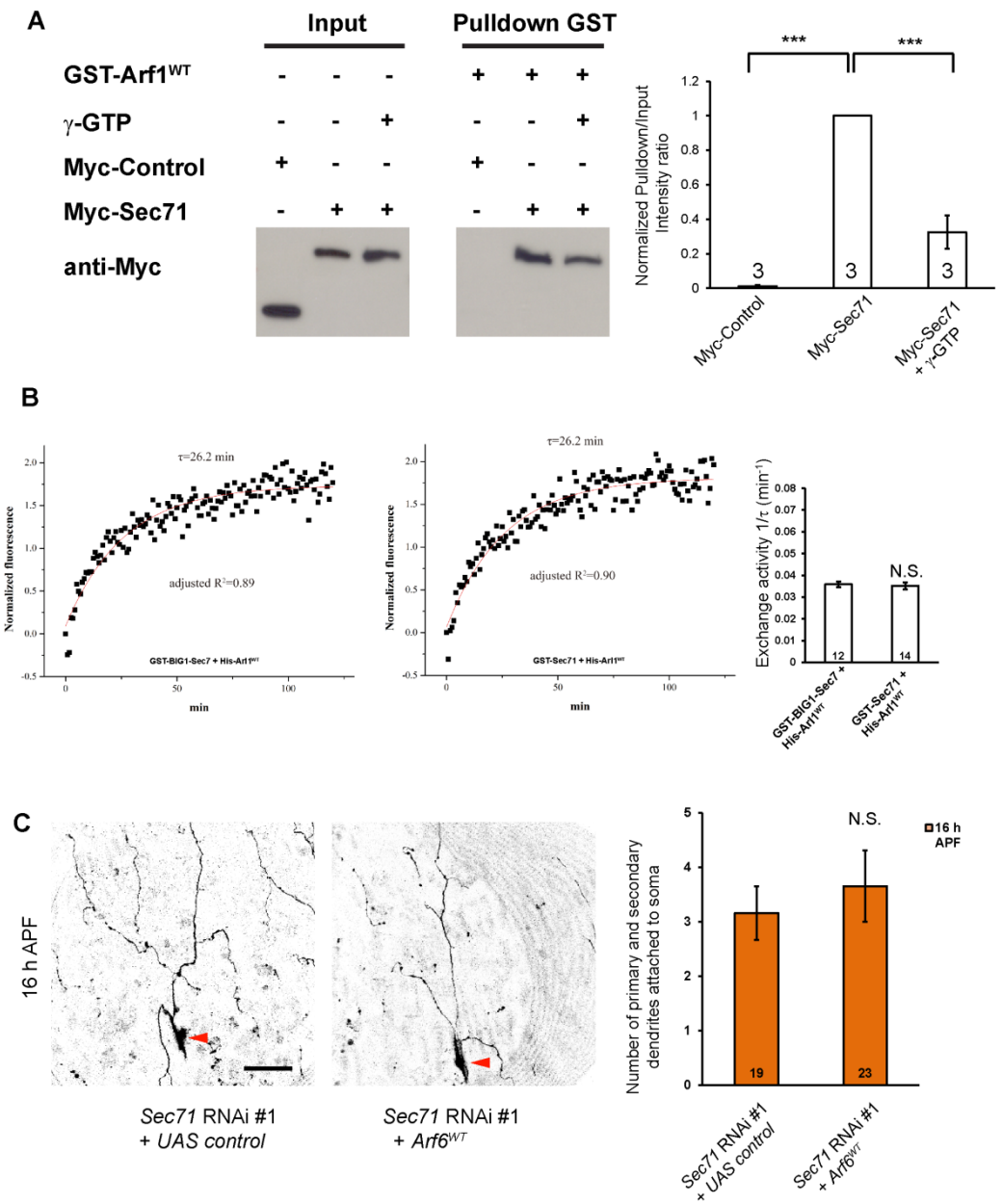

Figure S4. Sec71 is an Arf1GEF that preferentially interacts with GDP-bound Arf1.

(A) GST-Arf1^{WT} was associated with Myc-Sec71 but not with the Myc-tagged control protein, and this association was reduced in the presence of γ-GTP (n=3). Myc-tagged Sec71 and control protein were transfected and expressed in S2 cells. Error bars represent S.E.M.. ***p < 0.001 as assessed by one-way ANOVA and Bonferroni test. (B) Kinetics of fluorescence increases of GTP analog. Incubation of GST-tagged Sec7 domain of Sec71 (Sec71) led to slow kinetics towards Arl1, similar to the control GST-tagged Sec7 domain of hBIG1. Quantification of the exchange activity reflected by inverse of time constant, 1/τ value. N.S. not significant, as assessed by a Student's T-test. (C) The expression of Arf6^{WT} was unable to suppress the pruning defects in *Sec71* RNAi ddaC neurons at 16 h APF. Red arrowheads point to the ddaC somas. Quantification of the average number of primary and secondary ddaC dendrites. Scale bar in (C) represents 50 μm. Error bars represent S.E.M.. N.S. not significant, as assessed by two-tailed Student's T test. See genotypes in Supplemental list of fly strains.

Figure S5

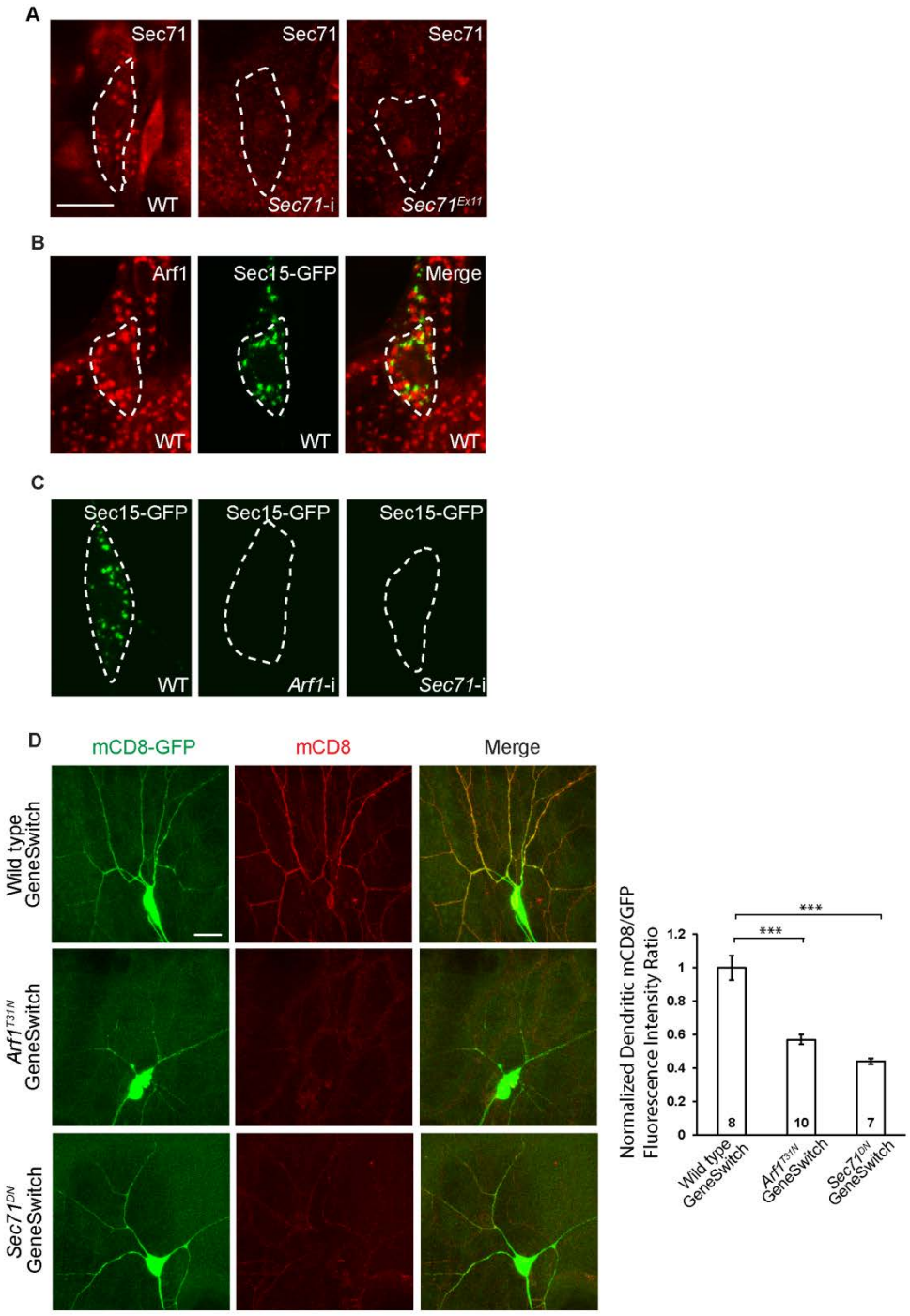

Figure S5. Arf1 and Sec71 regulate protein transport to the dendrite surface.

(A) Confocal images of wild-type and mutant ddaC neurons at the late wL3 stage immunostained with anti-Sec71. ddaC somas are marked by dashed lines. While Sec71 was distributed as punctate structures in wild-type ddaCs, Sec71 signals were completely abolished in *Sec71* RNAi #1 ddaC neurons and $Sec71^{Ex11}$ MARCM clones, verifying the specificity of the Sec71 antibody. (B) Sec15-positive puncta were localized adjacent to or partially colocalized with the Arf1-positive Golgi apparatus in wild-type ddaC neurons. (C) Sec15-GFP puncta were disrupted in *Arf1* RNAi and *Sec71* RNAi knockdown ddaC neurons, compared to the wild type. ddaC somas are marked by dashed lines. (D) mCD8 signals on the surface of the dendrites in wild-type ddaC neurons were detected by the antibody against its extracellular epitope in the detergent-free condition. However, the mCD8 signals were greatly reduced in $Sec71^{DN}$, and $Arf1^{T31N}$ expressing ddaC neurons. The graph represents quantification of normalized dendritic mCD8/GFP intensity. The scale bars represent 10 μm in (A) and 20 μm in (D). Error bars represent S.E.M.. ***$p < 0.001$ as assessed by one-way ANOVA and Bonferroni test. See genotypes in Supplemental list of fly strains.

Figure S6

A

Sec71 antigen		Dendrite Morpology	Dendrite Pruning Defect	TGN localization
DCB HUS Sec7 HDS1 HDS2 HDS3 HDS4	Sec71	Fully restored	Fully rescued	Yes
HUS Sec7 HDS1 HDS2 HDS3 HDS4	ΔDCB	Partially restored	Not rescued	No
DCB Sec7 HDS1 HDS2 HDS3 HDS4	ΔHUS	Further reduced	N.A.	Yes
DCB HUS Sec7 HDS2 HDS3 HDS4	ΔHDS1	Further reduced	N.A.	Yes
DCB HUS Sec7 HDS1	ΔHDS2-4	Fully restored	Fully rescued	Yes
DCB HUS Sec7 HDS1 HDS2	ΔHDS3-4	Fully restored	Fully rescued	Yes
DCB HUS Sec7 HDS1 HDS2 HDS3	ΔHDS4	Fully restored	Fully rescued	Yes

B

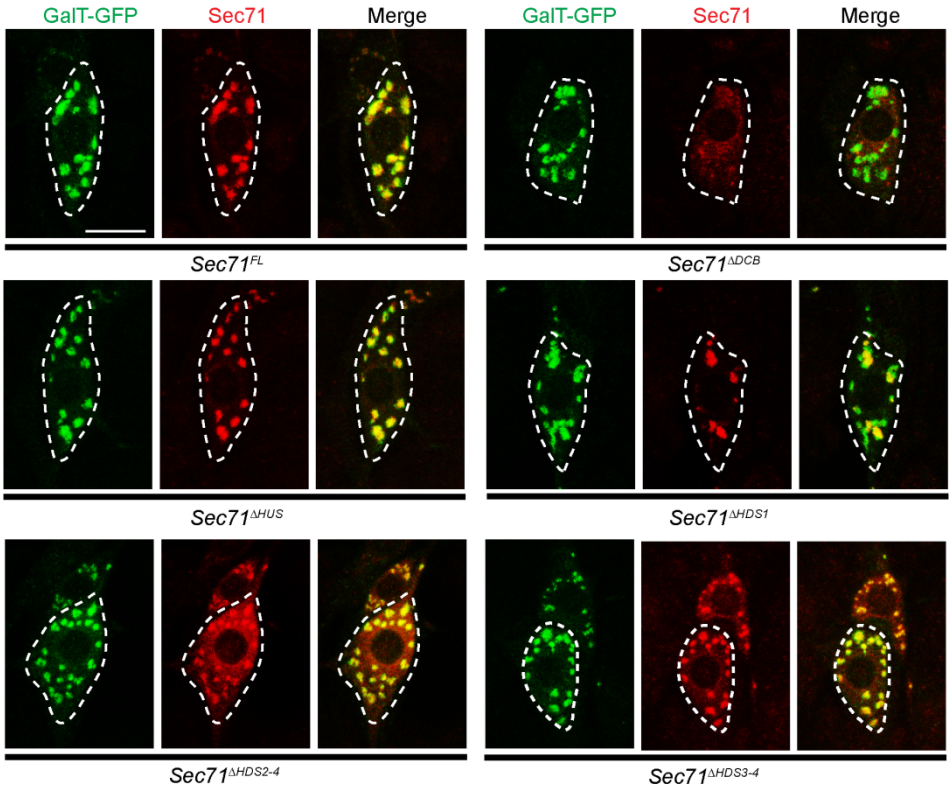

Figure S6. Structure-function analysis of the Sec71 protein.

(A) A summary of structure-function analysis of Sec71. Sec71 contains multiple domains: Dimerization/Cyclophilin Binding domain (DCB), Homology Upstream of Sec7 domain (HUS), Sec7 domain and Homology Downstream of Sec7 domain (HDS). (B) Confocal images of ddaC neurons at the late wL3 stage immunostained with anti-Sec71. Similar to full-length RNAi-resistant Sec71, Sec71$^{\Delta HUS}$, Sec71$^{\Delta HDS1}$, Sec71$^{\Delta HDS2\text{-}4}$ and Sec71$^{\Delta HDS3\text{-}4}$, but not Sec71$^{\Delta DCB}$, were localized on Golgi compartments labelled by GalT-GFP in ddaC neurons. Scale bar in (B) represents 10 μm. See genotypes in Supplemental list of fly strains.

Figure S7

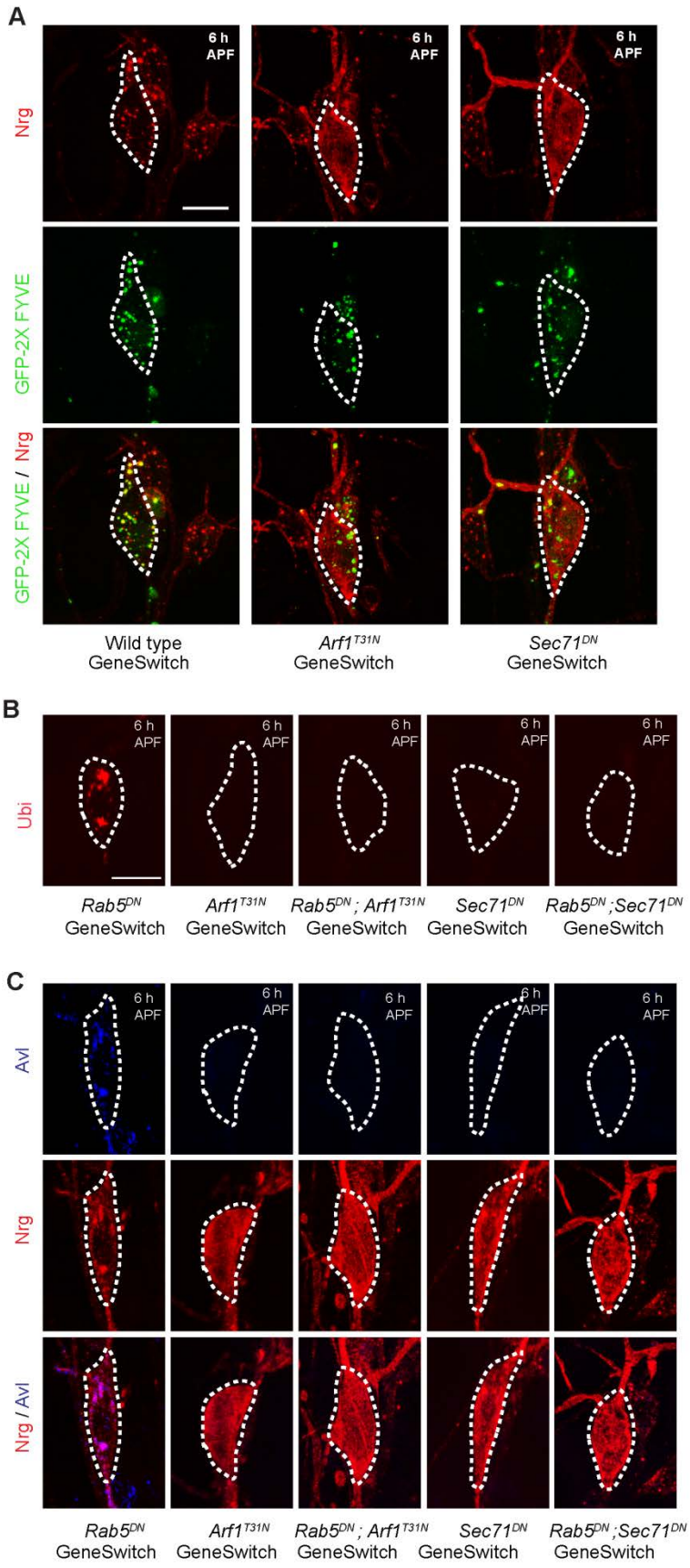

Figure S7. Arf1/Sec71-mediated secretory pathway is required for downregulation of the cell adhesion molecule Nrg prior to dendrite pruning

(A-C) Confocal images of ddaC neurons at 6 h APF stage immunostained for anti-Nrg (in red), anti-Ubiquitin (in red) or anti-Avl (in blue). (A) While Nrg proteins in wild-type ddaC neurons were redistributed to the early endosome labelled by GFP-2xFYVE at 6 h APF, Nrg in $Arf1^{T31N}$ or $Sec71^{DN}$-expressing ddaC neurons did not co-localize with those GFP-2xFYVE puncta and remained on the plasma membrane. (B) 2-3 ubiquitinated protein deposits were accumulated in $Rab5^{DN}$ expressing ddaC neurons but not in $Arf1^{T31N}$, $Rab5^{DN}$ and $Arf1^{T31N}$ co-expressing, $Sec71^{DN}$, or $Rab5^{DN}$ and $Sec71^{DN}$ co-expressing ddaC neurons at 6 h APF. (C) Avl/Nrg-positive aberrant endosomes were present in $Rab5^{DN}$ expressing ddaC neurons but absent in $Arf1^{T31N}$-expressing, $Rab5^{DN}$ and $Arf1^{T31N}$-co-expressing, $Sec71^{DN}$-expressing, or $Rab5^{DN}$ and $Sec71^{DN}$-co-expressing ddaC neurons at 6 h APF. ddaC somas are marked by dashed lines. The scale bars in (A) and (B) represent 10 μm. See genotypes in Supplemental list of fly strains.

Supplemental Material and Methods

Fly Strains

The following fly stocks were used in this study: *UAS-Rab5*^{DN} (M. Gonzalez-Gaitan)(Wucherpfennig et al., 2003), *UAS-GFP-Rab5* (M. Gonzalez-Gaitan)(Wucherpfennig et al., 2003), *UAS-Mical*$^{N\text{-}ter}$ (A. Kolodkin)(Terman et al., 2002), *UAS-GFP-2xFYVE* (M. Gonzalez-Gaitan)(Wucherpfennig et al., 2003), *ppk-Gal4* on II and III (Y. Jan) (Grueber et al., 2003), *SOP-flp (#42)* (a kind gift from T. Uemura), *UAS-Sec31-mCherry* (S. Luschnig)(Forster et al., 2010), *UAS-Sec15-GFP* (H. Bellen)(Jafar-Nejad et al., 2005), *UAS-Arf6*^{DN} (E. Chen), *UAS-Arf6* (E. Chen), *loner*^{T1032}(E. Olson)(Chen et al., 2003), *UAS-Step*^{DN} (T. Harris)(Lee and Harris, 2013), *Arl1*^{1} (J. Kennison)(Tamkun et al., 1991).

The following stocks were obtained from Bloomington Stock Center (BSC): *Gal4*$^{109(2)80}$, *elav-Gal4*, Control RNAi (BL#50613), *nrg* RNAi #1 (BL#38215), *nrg* RNAi #2 (BL#37496), *ppk-CD4-tdGFP* (BL#35843), *GSG2295-Gal4* (BL#40266), *Sec71* RNAi #1 (BL#32366), *UAS-GalT-GFP* (BL#30902), *UAS-Rab4-mRFP* (BL#8505), *UAS-mito-HA-GFP* (BL#8442).

The following Stocks were obtained from Vienna *Drosophila* RNAi Center (VDRC): *Sec71* RNAi #2 (v100300), *Arf1* RNAi #1 (v23082), *Arf1* RNAi #2 (v103572).

The following stocks were obtained from Kyoto Stock Center: *Sec71*^{GS16990} (#206863).

Generation of *Sec71* mutants

We crossed *Sec71*^{GS16990} flies with a fly strain carrying the Δ*2–3* transposase to induce imprecise excision. About 150 lines were established on the basis of the absence of the *w*+ marker. 56 lethal lines were isolated and subjected to genomic PCR and DNA sequencing analysis. The line with a 1461-bp deletion was named *Sec71*^{Ex11} (Figure S3A). The

Sec71^{GS16990} insertion line probably hopped from the original insertion site to the second intron and created this imprecise excision mutant.

Immunohistochemistry and antibodies

The following primary antibodies were used for immunohistochemistry at the indicated dilution: guinea pig anti-Avl (1:500; Yu Lab) (Zhang et al., 2014), rabbit anti-GM130 (1:200, Abcam ab52649), mouse anti-Ubiquitin (1:500; FK2, Enzo Life Sciences BML-PW0150-0100), mouse anti-Nrg (1:20, BP104, DSHB), rabbit anti-Lva antibody (1:1000, a gift from W. Sullivana)(Sisson et al., 2000), guinea pig anti-Arf1 (1:200, Yu Lab), mouse and guinea pig anti-Sec71 (1:200, Yu Lab), rabbit anti-GFP (1:1000, Invitrogen A11122), Cy3-, Cy5- or fluorescein isothiocyanate (FITC) conjugated secondary antibodies (Jackson Laboratories, Cat#: 111-165-003, 112-095-003, 111-175-003) were used at 1:400 dilution. For immunostaining, pupae or larvae were dissected in PBS and fixed with 4% formaldehyde for 20 min. Mounting was performed in VectaShield mounting medium, and the samples were directly visualized by confocal microscopy.

Generation of *Arf1, Sec71* and other transgenes

The *Arf1* and *Sec71* full-length cDNA were PCR from EST LD24904 and LD29171 (DGRC) into Topo Entry and pDonor, respectively (Life Tech). The dominant-negative variant of *Sec71* was generated by E677K site mutagenesis (Agilent Tech). The GDP-locked and GTP-locked constructs of *Arf1* were generated by T31N and Q71L site mutagenesis, respectively. Sec71 RNAi-resistant construct against Sec71 RNAi #1 was generated by site mutagenesis using following two primers CGTCATTTCGAATGGGTTTAAGTTCA ACGAGTCC and GGACTCGTTGAACTTAAAC CCATTCGAAATGACG.

The GATEWAY pTW vector containing the respective fragment of the cDNA were constructed by LR reaction (Life Tech) and several transgenic lines were established by the Bestgene Inc. An Arf1 RNAi-resistant cDNA was synthesized with a silent mutation on the

third base of each codon (First Base Tech), and was subjected to subcloning into pUAST and generation of transgenic lines. The *Sec71* variants were generated by site mutagenesis (Agilent Tech) and subcloned into pTWF-attB and targeted to the attP2 site.

The cDNA fragment encoding the aa 1-100 portion of rat ManII protein were amplified by PCR, subcloned into Topo entry and pTWV to generate ManII-Venus transgene (Bestgene Inc).

Arf1 and Sec71 antibody production

The cDNA fragment corresponding to the aa 60-345 fragment of Sec71 was amplified by PCR and verified by DNA sequencing. The product was expressed using the MBP expression vector (pMAL, NEB) and the purified protein was used to immunize guinea pigs and mice to generate antibodies against Sec71. The Arf1 full-length cDNA was amplified by PCR and verified by DNA sequencing. The product was expressed using the GST expression vector (pGEX 4T-1, Pharmacia) and the purified protein was used to immunize guinea pigs to generate antibodies against Arf1. The specificity of these antibodies was verified in respective RNAi and/or mutant ddaC neurons.

MARCM analysis of ddaC neurons

We carried out MARCM clonal analysis, dendrite imaging, and branch quantification as previously described (Kirilly et al., 2009). Briefly, ddaC or da clones were picked up and imaged at the WP stage according to their location and the dendritic arbor morphology. The same da neurons were examined for dendrite pruning defects at 16 h APF.

Co-Immunoprecipitation (Co-IP) and GST pull-down assay

We carried out S2 cell culture and Western blotting as described below. Myc-Sec71, Flag-Arf1^{WT}, Flag-Arf1^{T31N} and Flag-Arf1^{Q71L} expression vectors were generated by Gateway cloning and were transfected into S2 cells using Effectene Transfection Reagent (Qiagen). Transfected S2 cells were homogenized with the lysis buffer (25 mM Tris pH8/27.5 mM

NaCl/20 mM KCl/25 mM sucrose/1 mM DTT/10% (v/v) glycerol/0.5% Nonidet P40) with protease inhibitors (Complete, Boehringer; PMSF 10 µg/ml, Sodium orthovanadate 10 µg/ml). The supernatants were used for immunoprecipitation with anti-Myc (1:2,000, ab32, Abcam) overnight at 4°C, followed by incubation with protein A/G beads (Pierce Chemical Co.) for 2 h. Protein A/G beads were washed four times with cold PBS. Bound proteins were separated by SDS-PAGE and analysed by Western blotting with anti-Myc, anti-Flag HRP-conjugated antibody.

$Arf1^{WT}$, $Arf1^{T31N}$ and $Arf1^{Q71L}$ were inserted into (pGEX 4T-1, Pharmacia). The GST pull-down assays were carried out as previously described. Briefly, glutathione-sepharose 4B beads (GE Healthcare) bounded GST-Arf1 fusion protein were incubated for 3 h with Myc-Sec71protein extracts derived from S2 cell cultures, respectively. Bound beads were washed one time with the lysis buffer, two times with PBS and subjected to immunoblotting. γ–GTP (G0635, Sigma-Aldrich, 0.2mM) was pre-incubated with GST-Arf1 at room temperature for 30 min and also added into the lysis buffer. The blot bands were quantified in ImageJ software.

Trafficking Assay

eL3 staged larvae were fed with RU486 for 12 h. For immunostaining, larvae were dissected in PBS and fixed with 4% formaldehyde for 20 min. The fillets were incubated with rat monoclonal anti-CD8α (1:100, CALTAG Laboratories) in PBS and washed for three times with PBS in the detergent-free condition, which was followed by Cy3- secondary antibody incubation and wished for three times in the detergent-free condition. The intensity of immunofluorescence was measured in the same confocal setting for both mutant and control.

In vitro guanine nucleotide exchange assay

We carried out the in vitro guanine nucleotide exchange assays as previously described (Mahajan et al., 2013). GST fusion proteins for the Sec7 domain of Sec71 (aa554-790), its dominant negative form (E-K) and Sec7 domain of hBIG1 were expressed using the GST expression vector pGEB. 6xHis-tagged Arf1^{WT} and 6xHis-tagged Arl1^{WT} were expressed via the vector pET37b. The 6xHis-Arf1 fusion proteins were subjected to Tobacco Etch Virus protease cleavage to remove the N-terminal 6xHis-tag followed by gel filtration. All fusion proteins were dialyzed against HK buffer (50 mM HEPES pH 7.5, 120 mM KCl). The exchange assays were conducted in a black 96-well plate (Greiner Bio-One). Each reaction had 150 µl HKM buffer (HK buffer supplemented with 1 mM MgCl2 and 1 mM DTT) containing 1 µM Mant-GMPPNP, 1 µM 6xHis-Arf1^{WT}/6xHis-Arl1^{WT}, and 1 µM EDTA and 0.7 mM testing GST proteins (GST, GST-Sec71, GST-Sec71^{EK}, or GST-Sec7-hBIG1). The fluorescence was monitored by Tecan Infinite M200 pro at 25 °C with the excitation at 360 nm and emission at 440 nm. The fluorescence data were collected every 30 or 50 seconds depending on the total number of samples per plate. The exchange kinetic traces with significant spikes were rejected. Single exponential curve fitting were analyzed in OriginPro 8.5 (Origin Lab).

Quantification of immunolabeling

We quantified the immunolabeling intensities of Nrg at 6 h APF, as described previously (Zhang et al., 2014). Basically, soma/dendrite/axon contours were outlined on the individual fluorescent channel according to the GFP channel in ImageJ software. After subtracting the background (Rolling Ball Radius=50) on the entire image of that channel, we measured the mean grey value in the marked areas in ddaC or ddaE on the same images and calculated their ratios. The ratios were normalized to corresponding average control values and subjected to one-way ANOVA and Bonferroni tests for comparison between different conditions (*p<0.05, **p<0.01, ***p<0.001, n.s., not significant). Graphs display the average

values of ddaC/ddaE ratios and the standard error of means (S.E.M). The number of samples (n) in each group is shown on the bars.

Quantification of ddaC dendrites

Live confocal images of ddaC neurons expressing *UAS-mCD8-GFP* driven by *ppk-GAL4* were shown at WP and 16h APF. The average number of primary and secondary dendrites attached to soma was counted from wild type or mutant ddaC neurons. Primary dendrites are attached to the soma, while secondary dendrites are attached to the soma via their respective primary dendrites. The number of samples (n) in each group is shown on the bars. Statistical significance was determined using either two-tailed Student's T test (two samples) or one-way ANOVA and Bonferroni test (multiple samples) (*p<0.05, **p<0.01, ***p<0.001, n.s., not significant). Error represent S.E.M. Dorsal is up in all images.

Genotypes of fly strains

Figure 1: (B) *w*; ppk-Gal4, UAS-mCD8GFP / +; UAS-Dcr2 / UAS*-Control RNAi. (C) *w*; ppk-Gal4, UAS-mCD8GFP / +; UAS-Dcr2 / UAS-Arf1* RNAi #1. (D) *w*; ppk-Gal4, UAS-mCD8GFP, UAS-Dcr2 / +; UAS-Arf1* RNAi#1 / *UAS-Arf1(RNAi Resistant).* (E) *w*; ppk-Gal4 / UAS-Arf1^{T31N}; ppk-Gal4, UAS-mCD8GFP / +*. (F, G) *w*; UAS-Arf1^{T31N}/* GSG2295-*Gal4, ppk-tdGFP*. (H) *w*; UAS-Arf1^{Q71L} /* GSG2295-*Gal4, ppk-tdGFP*. (I) *w*; UAS-Arf1^{WT} /* GSG2295-*Gal4, ppk-tdGFP*.

Figure 2: (A-A") *w*; ppk-Gal4 / +; UAS-GalT-GFP / +*. (B-B") *w*; ppk-Gal4 / ppk-Gal4; ppk-Gal4, UAS-mCD8GFP / ppk-Gal4, UAS-mCD8GFP*. (C-C") *w*; ppk-Gal4 / +; UAS-Sec31-mCherry / +*. (D) *w*;* GSG2295-*Gal4 / UAS-Arf1^{T31N}; UAS-GalT-GFP / +*. (E) *w*; UAS-Arf1^{T31N}/* GSG2295-*Gal4, ppk-tdGFP* . (F) *w*;* GSG2295-*Gal4 / UAS-Arf1^{T31N}; UAS-Sec31-mCherry / +*. (G-G") *w*; ppk-Gal4, UAS-mCD8RFP, UAS-Dcr2 / +; UAS-ManII-Venus / +*. (H-H") *w*; ppk-Gal4, UAS-mCD8RFP, UAS-Dcr2 / +; UAS-ManII-Venus / UAS-Arf1* RNAi #1.

Figure 3: (A) *w*; ppk-Gal4, UAS-mCD8GFP / +; UAS-Dcr2 / UAS*-Control RNAi. (B) *w*; ppk-Gal4, UAS-mCD8GFP / +; UAS-Dcr2 / UAS-Sec71* RNAi #1. (C) *w*; ppk-Gal4, UAS-mCD8GFP, UAS-Dcr2 / +; UAS-Sec71(RNAi-Resistant) / UAS-Sec71* RNAi #1. (D) *w*; ppk-Gal4 / UAS-Sec71* RNAi #2*; ppk-Gal4, UAS-mCD8GFP / ppk-Gal4, UAS-mCD8GFP, UAS-Dcr2*. (E, F) *w*; UAS-Sec71^{DN} /* GSG2295-*Gal4, ppk-tdGFP* .

Figure 4: (G) *w*; ppk-Gal4, UAS-mCD8GFP, UAS-Dcr2 / +; UAS-Mical$^{N\text{-}ter}$ / UAS-Sec71* RNAi #1. (H) *w*; ppk-Gal4, UAS-mCD8GFP, UAS-Dcr2 / UAS-Arf1^{WT};UAS-Sec71* RNAi #1 / +.

Figure 5: (A-A") *w*; ppk-Gal4 / +; UAS-GalT-GFP / +*. (B-B") *w*; ppk-Gal4 / ppk-Gal4; ppk-Gal4, UAS-mCD8GFP / ppk-Gal4, UAS-mCD8GFP*. (C-C") *w*; ppk-Gal4 / ppk-Gal4; ppk-Gal4, UAS-mCD8GFP / ppk-Gal4, UAS-mCD8GFP*. (D-D") *w*; ppk-Gal4 / +; UAS-Sec31-mcherry / +*. (E) *w*;* GSG2295-*Gal4 / UAS-Sec71^{DN}; UAS-GalT-GFP / +*. (F) *w*; UAS-Sec71^{DN}* / GSG2295-*Gal4, ppk-tdGFP*. (G) *w*;* GSG2295-*Gal4 / UAS-Sec71^{DN}; UAS-Sec31-mcherry / +*. (H) *w*; ppk-Gal4 / ppk-Gal4; ppk-Gal4, UAS-mCD8GFP / ppk-Gal4, UAS-mCD8GFP*. (H') *w*; ppk-Gal4, UAS-mCD8GFP / +; UAS-Dcr2 / UAS-Sec71* RNAi #1. (H") *w*; UAS-Sec71^{DN}* / GSG2295-*Gal4, ppk-tdGFP* . (I) *w*; ppk-Gal4 / ppk-Gal4; ppk-Gal4, UAS-mCD8GFP / ppk-Gal4, UAS-mCD8GFP*. (I') *w*; ppk-Gal4, UAS-mCD8GFP / +; UAS-Dcr2 / UAS-Arf1* RNAi #1. (I") *w*; UAS-Arf1^{T31N}* / GSG2295-*Gal4, ppk-tdGFP* .

Figure 6: (B) *w*; ppk-Gal4, UAS-mCD8GFP, UAS-Dcr2; UAS-Mical$^{N\text{-}ter}$ / UAS-Sec71* RNAi #1. (C) *w*; ppk-Gal4, UAS-mCD8GFP, UAS-Dcr2 / +; UAS-Sec71 (RNAi-Resistant) / UAS-Sec71* RNAi #1. (D) *w*; ppk-Gal4, UAS-mCD8GFP, UAS-Dcr2 / +; UAS-Sec71$^{\Delta DCB}$ / UAS-Sec71* RNAi #1. (E) *w*; ppk-Gal4, UAS-mCD8GFP, UAS-Dcr2 / +; UAS-Sec71$^{\Delta HDS2\text{-}4}$ / UAS-Sec71* RNAi #1. (F) *w*; ppk-Gal4, UAS-mCD8GFP, UAS-Dcr2 / +; UAS-Sec71$^{\Delta HDS3\text{-}4}$ / UAS-Sec71* RNAi #1.

Figure 7: (A) *w*; ppk-Gal4 / ppk-Gal4; ppk-Gal4, UAS-mCD8GFP / ppk-Gal4, UAS-mCD8GFP*. (B) *w*; ppk-Gal4, UAS-Rab5^{DN} / +; ppk-Gal4, UAS-mCD8GFP / +*. (C) *w*; UAS-Arf1^{T31N}* / GSG2295-*Gal4, ppk-tdGFP*. (D) *w*; UAS-Sec71^{DN}* / GSG2295-*Gal4, ppk-tdGFP* . (F) *w*; ppk-Gal4, UAS-mCD8GFP, UAS-Dcr2 / +; UAS*-Control RNAi / *UAS-Arf1* RNAi #1. (G) *w*; ppk-Gal4, UAS-mCD8GFP, UAS-Dcr2 / UAS- nrg* RNAi *#1; UAS-Arf1* RNAi #1 / +. (H) *w*; ppk-Gal4, UAS-mCD8GFP, UAS-Dcr2 / UAS- nrg* RNAi *#2; UAS-Arf1* RNAi #1 / +. (J) *w*; ppk-Gal4, UAS-mCD8GFP, UAS-Dcr2 / +; UAS*-Control RNAi / *UAS-Sec71* RNAi #1. (K) *w*; ppk-Gal4, UAS-mCD8GFP, UAS-Dcr2 / UAS- nrg* RNAi *#1; UAS- Sec71* RNAi #1 / +. (L) *w*; ppk-Gal4, UAS-mCD8GFP, UAS-Dcr2 / UAS- nrg* RNAi *#2; UAS-Sec71* RNAi #1 / +.

Figure S1: (A) **Control:** *w*; ppk-Gal4, UAS-mCD8GFP / +; UAS-Dcr2 / UAS*-Control RNAi. ***Arf1* RNAi #2:** *w*; ppk-Gal4, UAS-mCD8GFP / UAS-Arf1* RNAi #2; *UAS-Dcr2 / +*. ***Arf1^{WT}*:** *w*; ppk-Gal4 / UAS-Arf1^{WT}; ppk-Gal4, UAS-mCD8GFP / +*. (B) **Wild type:** *w*; Gal4$^{109(2)80}$, UAS-mCD8GFP, SOP-flp / +; FRT82B / FRT82B, tubP-Gal80*. ***Arf1^{T31N}*:** *w*; Gal4$^{109(2)80}$, UAS-mCD8GFP, SOP-flp / UAS-Arf1^{DN}; FRT82B / FRT82B, tubP-Gal80*. **Wild type:** *w*;* GSG2295-*Gal4 / +; UAS-mCD8GFP / UAS-Mical$^{N\text{-}Ter}$*. ***Arf1^{T31N}*:** *w*;* GSG2295-*Gal4 / UAS-Arf1^{T31N}; UAS-mCD8GFP / +*. ***Arf1* RNAi #1:** *w*; ppk-Gal4, UAS-mCD8GFP / +; UAS-Dcr2 / UAS-Arf1* RNAi #1. (C) **Wild type:** *w*;; ppk-Gal4, UAS-mCD8GFP / ppk-Gal4, UAS-mCD8GFP*. ***Arf6^{DN}*:** *w*; ppk-Gal4 / UAS-Arf6^{DN}; ppk-Gal4, UAS-mCD8GFP / +*. ***Arl1^{1}:*** *w*; ppk-Gal4, UAS-mCD8GFP, SOP-flp #42/+; Arl1^{1},FRT2A/ tubP-Gal80,FRT2A*. (D) **Control RNAi:** *w*; ppk-Gal4, UAS-mCD8GFP / +; UAS-Dcr2 / UAS*-Control RNAi.

***Arf1* RNAi #1:** *w*; ppk-Gal4, UAS-mCD8GFP / +; UAS-Dcr2 / UAS-Arf1* RNAi #1. ***Sec71* RNAi #1:** *w*; ppk-Gal4, UAS-mCD8GFP / +; UAS-Dcr2 / UAS- Sec71* RNAi #1.

Figure S2: (A) **Wild type:** *w*; ppk-Gal4, UAS-mCD8GFP / ppk-Gal4, UAS-mCD8GFP; UAS-Dcr2 / UAS-Dcr2*. ***Arf1* RNAi #1**: *w*; ppk-Gal4, UAS-mCD8GFP / +; UAS-Dcr2 / UAS-Arf1* RNAi #1. ***Arf1* RNAi #2**: *w*; ppk-Gal4, UAS-mCD8GFP / UAS-Arf1* RNAi #2; *UAS-Dcr2 / +*. (B) *w*; ppk-Gal4 / ppk-Gal4; ppk-Gal4, UAS-mCD8GFP / ppk-Gal4, UAS-mCD8GFP*. (C) *w*; ppk-Gal4 / UAS-Rab4-mRFP*. (D) *w*; ppk-Gal4 / UAS-GFP-Rab5*. (E) *w*; ppk-Gal4 / UAS-mito-HA-GFP*. (F**) Wild type:** *w*; ppk-Gal4, UAS-mCD8RFP, UAS-Dcr2 / +; UAS-GalT-GFP / +*. ***Arf1* RNAi**: *ppk-Gal4, UAS-mCD8RFP, UAS-Dcr2 / +; UAS-GalT-GFP / UAS-Arf1* RNAi #1. ***Sec71* RNAi**: *ppk-Gal4, UAS-mCD8RFP, UAS-Dcr2 / +; UAS-GalT-GFP / UAS-Sec71*RNAi #1. (G) *w*; ppk-Gal4, UAS-mCD8RFP, UAS-Dcr2 / +; UAS-GalT-GFP / +*. (H) *w*; ppk-Gal4, UAS-mCD8RFP, UAS-Dcr2 / +; UAS-GalT-GFP / UAS-Arf1* RNAi #1.

Figure S3: (B) ***Sec71*^{Ex11}:** *w*; Sec71^{Ex11}, FRT40A / tubP-Gal80, FRT40A; ppk-Gal4, UAS-mCD8GFP, SOP-flp / +*. ***Sec71*^{Ex11} Rescue:** *elav-Gal4, UAS-mCD8GFP, hs-FLP, w* / Gal4$^{5-40}$, UAS-Venus:pm, SOP-flp #42 ; Sec71^{Ex11}, FRT40A / tubP-Gal80, FRT40A; UAS-Sec71^{FL} / +*. (C) **Wild type:** *w*; Gal4$^{109(2)80}$, UAS-mCD8GFP, SOP-flp / +; FRT82B / FRT82B, tubP-Gal80*. ***Sec71*^{DN}:** *w*; Gal4$^{109(2)80}$, UAS-mCD8GFP, SOP-flp / UAS-Sec71^{DN}; FRT82B / FRT82B, tubP-Gal80*. (D) **Wild type:** *w*;* GSG2295-*Gal4 / +; UAS-mCD8GFP / UAS-Mical^{N-Ter}*. ***Sec71*^{DN}:** *w*;* GSG2295-*Gal4 / UAS-Sec71^{DN}; UAS-mCD8GFP / +*. ***loner*^{T1032}:** *elav-Gal4, UAS-mCD8GFP, hs-FLP, w* / Gal4$^{5-40}$, UAS-Venus:pm, SOP-flp #42;; FRT82B, loner^{T1032} / FRT82B, tubP-Gal80*. ***Step*^{DN}:** *w*; ppk-Gal4 / +; ppk-Gal4, UAS-mCD8GFP / UAS-step^{DN}*. (E) **Control RNAi:** *w*; ppk-Gal4, UAS-mCD8GFP / +; UAS-Dcr2 / UAS-Control* RNAi. ***Sec71* RNAi #1:** *w*; ppk-Gal4, UAS-mCD8GFP / +; UAS-Dcr2 / UAS-Sec71* RNAi #1.

Figure S4: (C) ***Sec71* RNAi #1+UAS control:** *w*; ppk-Gal4, UAS-mCD8GFP, UAS-Dcr2 / +; UAS-Mical^{N-ter} / UAS-Sec71* RNAi #1. ***Sec71* RNAi #1 + *Arf6*^{WT}:** *w*; ppk-Gal4, UAS-mCD8GFP, UAS-Dcr2 / UAS-Arf6^{WT};UAS-Sec71* RNAi #1 / +.

Figure S5: (A)**Wild type:** *w*; ppk-Gal4, UAS-mCD8GFP / ppk-Gal4, UAS-mCD8GFP; UAS-Dcr2 / UAS-Dcr2*. ***Sec71* RNAi #1**: *w*; ppk-Gal4, UAS-mCD8GFP / +; UAS-Dcr2 / UAS-Sec71* RNAi #1. ***Sec71*^{Ex11}:** *w*; Sec71^{Ex11}, FRT40A / tubP-Gal80, FRT40A; ppk-Gal4, UAS-mCD8GFP, SOP-flp / +*. (B) **Wild type**: *w*; ppk-Gal4 / UAS-Sec15-GFP*. (C) **Wild type**: *w*; ppk-Gal4, UAS-Dcr2 / UAS-Sec15-GFP*. ***Arf1* RNAi:** *w*; ppk-Gal4, UAS-Dcr2 / UAS-Sec15-GFP; UAS-Arf1* RNAi #1 / +. ***Sec71* RNAi:** *w*; ppk-Gal4 / UAS-Sec15-GFP; UAS-Sec71* RNAi #1 / +. (D) **Wild type:** *w*;* GSG2295-*Gal4 / +; UAS-mCD8GFP / UAS-Mical^{N-Ter}*. ***Arf1*^{T31N}:** *w*;* GSG2295-*Gal4 / UAS-Arf1^{T31N}; UAS-mCD8GFP / +*. ***Sec71*^{DN}:** *w*;* GSG2295-*Gal4 / UAS-Sec71^{DN}; UAS-mCD8GFP / +*.

Figure S6: (B) ***Sec71*^{FL}:** *w*; ppk-Gal4 / +; UAS-GalT-GFP / UAS-Sec71* (RNAi-Resistant). ***Sec71*$^{\Delta DCB}$:** *w*; ppk-Gal4 / +; UAS-GalT-GFP / UAS-Sec71$^{\Delta DCB}$*. ***Sec71*$^{\Delta HUS}$:** *w*; ppk-Gal4 /*

+; UAS-GalT-GFP / UAS-Sec71$^{\Delta HUS}$. ***Sec71$^{\Delta HDS1}$:*** *w*; ppk-Gal4 / +; UAS-GalT-GFP / UAS-Sec71$^{\Delta HDS1}$.* ***Sec71$^{\Delta HDS2-4}$:*** *w*; ppk-Gal4 / +; UAS-GalT-GFP / UAS-Sec71$^{\Delta HDS2-4}$.* ***Sec71$^{\Delta HDS3-4}$:*** *w*; ppk-Gal4 / +; UAS-GalT-GFP / UAS-Sec71$^{\Delta HDS3-4}$.*

Figure S7: (A) **Wild type:** *w*;* GSG2295-*Gal4 / +; UAS-GFP-2×FYVE / UAS-Mical^{N-Ter}.* ***Arf1^{T31N}:*** *w*;* GSG2295-*Gal4 / UAS-Arf1^{T31N}; UAS-GFP-2×FYVE / +.* ***Sec71^{DN}:*** *w*;* GSG2295-*Gal4 / UAS-Sec71^{DN}; UAS-GFP-2×FYVE / +.* (B-C) ***Rab5^{DN}:*** *w*; UAS-Rab5^{DN} /* GSG2295-*Gal4; ppk-tdGFP / UAS-Mical^{N-Ter}.* ***Arf1^{T31N}:*** *w*; UAS-Arf1^{T31N} /* GSG2295-*Gal4; ppk-tdGFP / UAS-Mical^{N-Ter}.* ***Rab5^{DN}; Arf1^{T31N}:*** *w*; UAS-Arf1^{T31N} /* GSG2295-*Gal4, UAS-Rab5^{DN}; ppk-tdGFP / +.* ***Sec71^{DN}:*** *w*; UAS-Sec71^{DN} /* GSG2295-*Gal4; ppk-tdGFP / UAS-Mical^{N-Ter}.* ***Rab5^{DN}; Sec71^{DN}:*** *w*; UAS-Sec71^{DN} /* GSG2295-*Gal4, UAS-Rab5^{DN}; ppk-tdGFP / +.*

Supplemental References

Chen, E. H., Pryce, B. A., Tzeng, J. A., Gonzalez, G. A. and Olson, E. N. (2003). Control of myoblast fusion by a guanine nucleotide exchange factor, loner, and its effector ARF6. ***Cell*** **114, 751-62.**

Forster, D., Armbruster, K. and Luschnig, S. (2010). Sec24-dependent secretion drives cell-autonomous expansion of tracheal tubes in Drosophila. ***Curr Biol*** **20, 62-8.**

Grueber, W. B., Jan, L. Y. and Jan, Y. N. (2003). Different levels of the homeodomain protein cut regulate distinct dendrite branching patterns of Drosophila multidendritic neurons. ***Cell*** **112, 805-18.**

Jafar-Nejad, H., Andrews, H. K., Acar, M., Bayat, V., Wirtz-Peitz, F., Mehta, S. Q., Knoblich, J. A. and Bellen, H. J. (2005). Sec15, a component of the exocyst, promotes notch signaling during the asymmetric division of Drosophila sensory organ precursors. ***Dev Cell*** **9, 351-63.**

Kirilly, D., Gu, Y., Huang, Y., Wu, Z., Bashirullah, A., Low, B. C., Kolodkin, A. L., Wang, H. and Yu, F. (2009). A genetic pathway composed of Sox14 and Mical governs severing of dendrites during pruning. ***Nat Neurosci*** **12, 1497-505.**

Lee, D. M. and Harris, T. J. (2013). An Arf-GEF regulates antagonism between endocytosis and the cytoskeleton for Drosophila blastoderm development. ***Curr Biol*** **23, 2110-20.**

Mahajan, D., Boh, B. K., Zhou, Y., Chen, L., Cornvik, T. C., Hong, W. and Lu, L. (2013). Mammalian Mon2/Ysl2 regulates endosome-to-Golgi trafficking but possesses no guanine nucleotide exchange activity toward Arl1 GTPase. ***Sci Rep*** **3, 3362.**

Sisson, J. C., Field, C., Ventura, R., Royou, A. and Sullivan, W. (2000). Lava lamp, a novel peripheral golgi protein, is required for Drosophila melanogaster cellularization. ***J Cell Biol*** **151, 905-18.**

Tamkun, J. W., Kahn, R. A., Kissinger, M., Brizuela, B. J., Rulka, C., Scott, M. P. and Kennison, J. A. (1991). The arflike gene encodes an essential GTP-binding protein in Drosophila. ***Proc Natl Acad Sci U S A*** **88, 3120-4.**

Terman, J. R., Mao, T., Pasterkamp, R. J., Yu, H. H. and Kolodkin, A. L. (2002). MICALs, a family of conserved flavoprotein oxidoreductases, function in plexin-mediated axonal repulsion. ***Cell*** **109, 887-900.**

Wucherpfennig, T., Wilsch-Brauninger, M. and Gonzalez-Gaitan, M. (2003). Role of Drosophila Rab5 during endosomal trafficking at the synapse and evoked neurotransmitter release. ***J Cell Biol*** **161, 609-24.**

Zhang, H., Wang, Y., Wong, J. J., Lim, K. L., Liou, Y. C., Wang, H. and Yu, F. (2014). Endocytic pathways downregulate the L1-type cell adhesion molecule neuroglian to promote dendrite pruning in Drosophila. ***Dev Cell*** **30, 463-78.**